Polyhedron 257 (2024) 117022

Contents lists available at ScienceDirect

Polyhedron

journal homepage: www.elsevier.com/locate/poly

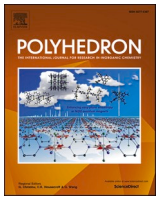

Green synthesis of *Abutilon indicum* (L) derived iron oxide (FeO) nanoparticles with excellent biological, anticancer and photocatalytic activities

Chellasamy Panneerselvam [a,b,*], Mohammed Ali Alshehri [a], Ahmed Saif [c], Uzma Faridi [d], Syed Khasim [e,f], Zuhair M Mohammedsaleh [g], Humaira Parveen [h], Noha Omer [h], Abdulrahman Alasmari [a], Sayeed Mukhtar [h], Hatem A. Al-Aoh [h]

[a] *Department of Biology, Faculty of Science, University of Tabuk, Tabuk 71491, Saudi Arabia*
[b] *Biodiversity Genomic Unit, Faculty of Science, University of Tabuk, Tabuk 71491, Saudi Arabia*
[c] *Department of Clinical Laboratory Science, Central Research Laboratory, College of Applied Medical Science, King Khalid University, Abha 61321, Saudi Arabia*
[d] *Department of Biochemistry, Faculty of Science, University of Tabuk, Tabuk 71491, Saudi Arabia*
[e] *Department of Physics, Faculty of Science, University of Tabuk, Tabuk 71491, Saudi Arabia*
[f] *Advanced Materials Laboratory, Department of Physics, Faculty of Science, University of Tabuk, Tabuk 71491, Saudi Arabia*
[g] *Department of Medical Laboratory Technology, Faculty of Applied Medical Sciences, University of Tabuk, Tabuk 71491, Saudi Arabia*
[h] *Department of Chemistry, Faculty of Science, University of Tabuk, Tabuk 71491, Saudi Arabia*

ARTICLE INFO

Keywords:
Green synthesis
A. indicum
Antibacterial effect
Anti-inflammatory activity
Anticancer activity

ABSTRACT

Cancer is one of the most common causes of death all over the world. Although there are many treatments available none of them are without side-effect and most of them are very expensive. Similarly, Inflammation is one of another common medical condition worldwide but most of the therapies available are not environment and pocket friendly. Thus, the aim of our study was to synthesize environmentally friendly, cost-effective FeO NPs with significant anticancer, anti-inflammatory, antibacterial properties. The green synthesis of Iron Oxide Nanoparticles (FeO NPs) using plant extract is one of the environmentally friendly, cost-effective, and a secure alternative to physical or chemical synthesis methods. In the present study we used *Abutilon indicum* leaf extract to synthesize the Ai-FeO NPs and performed various experiments to confirm the therapeutic potential of green synthesized Ai-FeO nanoparticles. In this method, an aqueous plant leaf extract (*A. indicum*: Ai) was used as a reducing and stabilizing agent for the synthesis of FeO nanoparticles. The synthesized Ai-FeO NPs were characterized by the ultraviolet–visible (UV–Vis) absorbance of the surface at a resonance band 415 nm. Fourier transform infrared (FTIR) spectroscopy study confirmed the inherent bioactive functional groups as capping and stabilizing agents for Ai-FeO NPs. The X-ray powder diffraction (XRD) spectra revealed crystalline nature of the NPs. Further, the synthesized NPs have been isolated in highly stable, crystalline nature with spherical shape having size 10–95 nm. In addition, the green synthesized Ai-FeO-NPs demonstrated dose-dependent antimicrobial, antioxidant, anti-inflammatory, and anticancer properties. The findings of this study suggested that *A. indicum* leaf extract mediated FeO nanoparticles could be potentially used as a therapeutic agent for many human diseases and breast cancer.

1. Introduction

According to World Health Organization, cancer is one of the leading causes of death, and the death rate is approximately 9 million in 2018 [1]. However, middle- and low-income nations account for 70 % of cancer deaths worldwide [1,2]. Inflammation, another medical condition, is among some of the most common medical issues worldwide. Fortunately, inflammation is an essential part of the healing process and maintains cellular function. However, acute, and chronic inflammations that are recognized could be problematic if not treated early [3]. The acute inflammation symptoms include redness, swelling, and pain inside tissues and joints [4]. Since both of the above-mentioned

* Corresponding author.
E-mail address: cpselva@ymail.com (C. Panneerselvam).

https://doi.org/10.1016/j.poly.2024.117022
Received 20 January 2024; Accepted 2 May 2024
Available online 3 May 2024

diseases are very common across the globe, there is an urgent need for new treatments methods that involve minimum cost and low or no side effects.

In recent years, nanotechnology has emerged as an important area of research in the fields of medicine and health. In the past few years, nanomedicine has revolutionized health care in many ways, and has many opportunities in a wide variety of sectors and scientific fields [5]. Nowadays, physical, chemical, and green methods are used for metallic nanoparticles synthesis. The use of chemical and physical methods comprises the formation of toxic chemical, high pressure, radiation, and involves costly equipment, results in a large quantity of chemical waste as a by-product. These waste chemical by-products could be hazardous to the environment [6,7]. Green synthesis of nanoparticles by using plant parts through biological methods is one of the very effective techniques, which results in higher yield than the other related techniques [8]. Plant components in the green synthesis play a crucial role as reducing and stabilizing agents along with other biochemical properties [9–11]. The green synthesis of metal and metal oxide nanoparticles is a novel method that avoids harmful chemicals, high cost and environmental contamination [12]. As a result, researchers are focussing on green approaches for producing nanoparticles from plants, microbes, and other biomaterials [8–13].

Plant extracts are easier way to synthesize metal oxide nanoparticles than microbial cultures because plant extracts don't require sterilized conditions to grow [10,11]. Usually, plant extracts contain phytochemicals including sugars, and several secondary metabolites such as polyphenols, flavonoids, terpenoids, phenolic acids, alkaloids, and protein, which causes the reduction and stabilization of metal nanoparticles [10]. Green synthesized NPs are promising antibacterial and anticancer agents and are safer, cost-effective medications than other commercial drugs [2,14]. Recent efforts have been focused on synthesising environmentally friendly NPs such as Ag, Au, Cu, CuO, ZnO, Se and Fe, which have been integrated into a variety of biological activities [15,16]. Among the various metal nanoparticles, scientists have been paying significant attention to FeO-NPs due to its most appealing properties as a multifunctional material. FeO-NPs have received extensive research attention in a variety of fields, including plant growth regulators, sensors, photocatalysts, fine ceramics, water treatment, pigments, electrochemical cells, and anticorrosive chemicals [17–21]. The FeO NPs have a wide variety of commercial applications including, biomedicine, vaccines, diagnostics, radiology, pathogens, enzymes, and cosmetics [22]. Further, these FeO NPs are typically utilised for many purposes, such as the removal of heavy metals, dyes, and antibiotics from water sources, as well as in the biomedical area for targeted drug delivery to the cancer cells [23,24]. Due to their propensity to generate highly reactive oxygen species, iron oxide nanoparticles have been effective against a wide range of pathogenic bacterial strains and fungi [16]. Recently, researchers are focussing on green synthesis FeO NPs from various plant parts, for example the leaf extract of *Rhamnus triquetra* [25], *Platanus orientalis* leaf extract [26], *Madhuca indica* leaf extract [27], fruit extract of *Cynometra ramiflora* [28], *Carica papaya* leaf extract [20], *Hibiscus rosa sinensis* flower extract [14] and *Punica graatum* seeds extract [29], etc.

In the present study, FeO NPs were synthesized by green chemistry approach from *Abutilon indicum* (Malvaceae) plant parts which contains a variety of phytochemical such as alkaloids, proteins and amino acids, flavonoids, steroids, glycosides, saponins. The crude leaf extract of this plant had significant antioxidant, antibacterial, and anticancer activity [30–32]. Although *A. indicum* leaf extract is already reported to be used as reducing agent in the previous research to synthesize silver NPs [33], ZnO NPs [34], CuO NPs [35], MnO NPs [36], and Ni nanoparticles [37], but there are only few reports on the synthesis of FeO NPs from *A. indicum* leaf extract and their biological and photocatalytical properties.

Therefore, the present study focused on green synthesis of FeO NPs by using *A. indicum* leaf extract. Physical and chemical properties of the synthesized FeO NPs were analyzed using UV–visible (UV–Vis) spectroscopy, XRD, FTIR, HR-TEM, EDAX, Zeta potential analysis. Also, we evaluate their antioxidant, antibacterial, anti-diabetic, anti-inflammation, and anticancer activity. Hence, this research not only demonstrates the green synthesis of FeO NPs but also illustrates the multifunctional application of such synthesized FeO NPs.

2. Materials and methods

2.1. Chemicals

Ferric acetate basic (hydrous), nutrient agar and broth, 2,2-diphenyl-1-picrylhydrazyl (DPPH), hydrogen peroxide, 2 −Azino-bis (3-ethylbenzo-thiazoline-6-sulphonic acid) diammonium salt (ABTS), ascorbic acid, Acridine Orange/Ethidium bromide staining kit (AO/EB), 3-(4,5-dimethylthiazolyl-2-yl)-2, sodium nitroprusside, 5-diphenyl tetrazolium bromide (MTT).

2.2. Plant extracts preparation

Abutilon indicum leaf extracts were prepared according to the methods demonstrated by Venkatesan et al. [38] with slight modifications. 150 mL of deionized water and 5 g of *Abutilon indicum* leaf powder were combined and heated to 70 °C for one hour. Then the extracts were cooled at room temperature and separated with Whatman No. 1filter paper. At the end the extracted solution was used to produce nanoparticles.

2.3. Green chemistry synthesis and characterization of Ai-FeO NPs

For the synthesis of Ai-FeO NPs, Abbasi et al. [23] method was adopted with slight modification. 100 mL of *A. indicum* leaf extract and 6 g of ferric acetate basic (hydrous) were combined to produce FeO NPs. The mixture was kept on a hot plate and heated continuously for two hours at 70 °C. The color of the solution changed from yellow to blackish after 2 hr, indicating the formation of FeO NPs. It was then cooled at room temperature. The powder at the bottom was retained, once the solution was centrifuged for 10 min at 12,000 rpm, Further, it was washed thrice with distilled water to remove all unreacted biological species from the residue. In the next step, the samples were washed with ethanol and calcinated for three hours at 400 °C to obtain the Ai-FeO NPs.

The green synthesized iron oxide nanoparticles were analyzed by UV–VIS light spectra (Jasco UV-650, Japan). The synthesized materials' purity and crystalline phase were examined using a Model D8, BRUKER AXS, and Cu K radiation ($\lambda = 0.15425$ nm), in the range of 20° to 80°. The sizes and structure of Ai-FeO NPs were confirmed by transmission electron microscopy (TEM, Zeiss-EM10C). Additionally, their elemental mapping was examined using EDS (FE-SEM with EDS, Carl Zeiss- Sigma model, Germany), and stability using zeta potential with the help of Malvern analyser (Model- Nano-ZS90). FTIR (in the range The 400–4000 cm^{-1}) was used to characterize the capping agents of the leaf extract, while synthesizing Ai-FeO NPs.

2.4. Antioxidant activity of green synthesized FeO NPs

In vitro antioxidant assays including DPPH (2,2-diphenyl-1-picrylhydrazyl), reducing potential and Nitric oxide scavenging property of FeO NPs, Ascorbic acid at different dosage such as 20, 40, 60, 80, 100 and 120 μg/ml, was determined by UV–VIS spectrophotometer using different wavelength such as 515 nm for DPPH, 700 nm for ABTS and 546 nm for NO assays [39,40].

2.5. Antibacterial activity of FeO NPs

The bactericidal potential of *A. indicum* leaf extract and Ai-FeO NPs

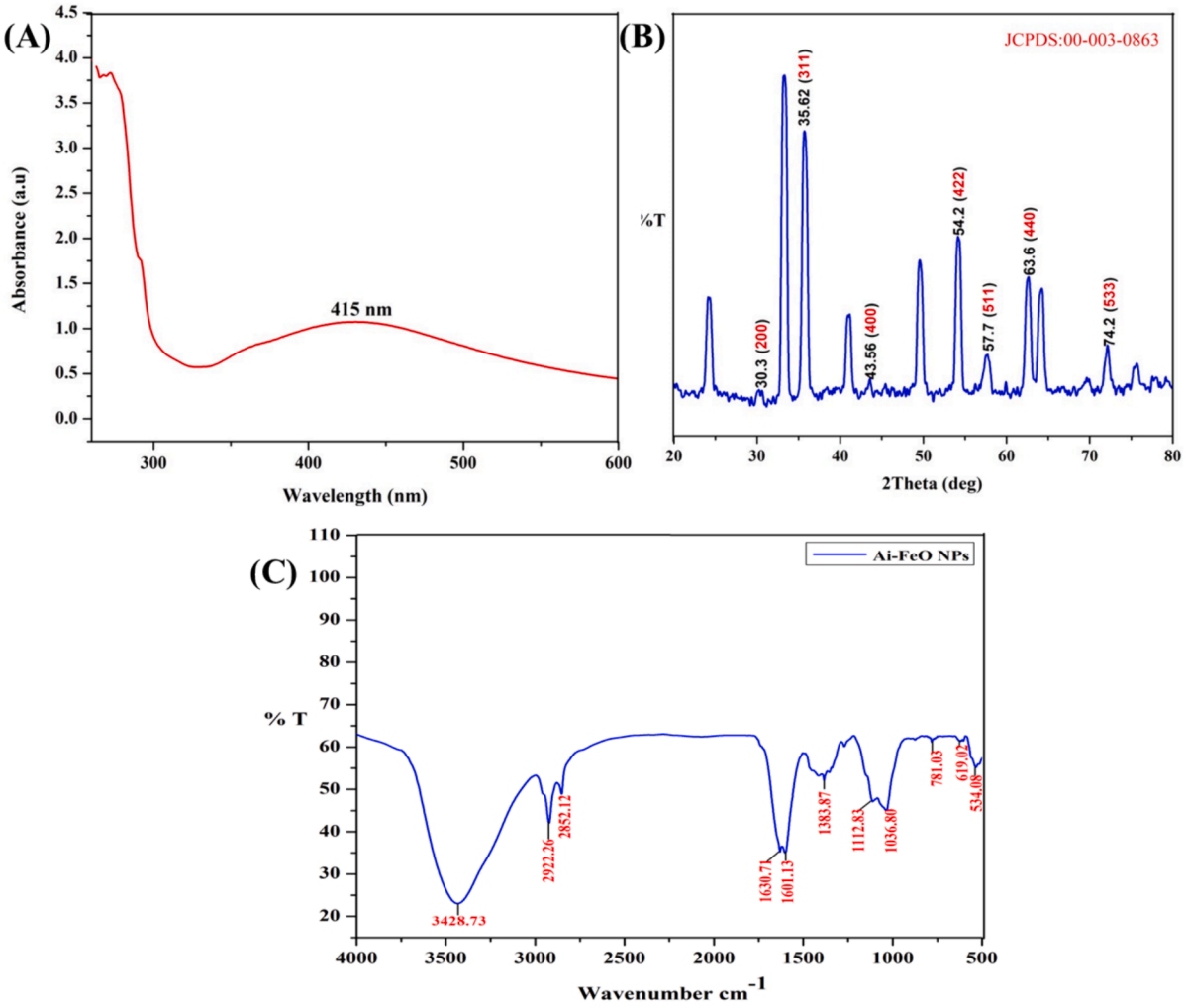

Fig. 1. (**A**) UV–vis spectrum of *Abutilon indicum*-synthesized FeO NPs; (**B**) XRD pattern of Ai-FeO NPs; (**C**) Fourier transform infrared (FTIR) spectroscopy of FeO NPs using *A. indicum.*

was assessed by using the previously developed agar well diffusion method [40,41]. Antibacterial activity was assessed using clinically isolated gram + ve bacteria (*S. aureus, B. subtilis*), as well as gram-ve (*E. coli, P. aeruginosa*) bacteria. 100 µl of mature cultures that were 24 h old were swabbed onto the nutrient agar medium using an L-shaped rod. Further, the wells were created (6 mm) by sterile cork borer. The next step involved the study of various Ai-FeO NPs concentration (25, 50, 75, 100 µg/ml) on different bacterial strains. After swabbing, the plates were incubated at 37 °C for 24 h, and their Zone of Inhibition (mm) values were periodically assessed.

2.6. In vitro anti-inflammatory activity

In vitro anti-inflammation assays were carried out by following the method of Rajakumar et al. [42] with slight modification. Herein, we examined 5 mL of 1 % bovine serum albumin and Ai-FeO NPs, and diclofenac at different dosage like 20, 40, 60, 80,100 and 120 µg/ml, and the activity was determined by UV–vis spectrophotometer using different wavelength such as 540 nm for α-amylase, 660 nm for protein inhibitory assays.

2.7. Cytotoxic activity using MTT assay

MTT assay was used to demonstrate the cell viability of green synthesized Ai-FeO NPs, DOX. Breast cancer cells (MDA-MB-231) were injected into the 96-well plates. Then the cancer cells treated with varying concentration of DOX, Ai-FeO NPs (20 to 120 µg/ml) for 24 h at 37 °C. Following incubation, the OD was analyzed at 570 nm, and the IC_{50} values were calculated [43].

2.7.1. Dual staining (AO/EB) and DAPI analysis of apoptosis

The apoptosis related morphological characteristic features were analyzed by staining the cells with acridine orange and ethidium bromide (AO/EB), as well as 4′,6-Diamidino-2-phenylindole dihydrochloride (DAPI). We determined the IC_{50} of Ai-FeO NPs after the cells were sown in six-well plates for 48 h. Then twenty micro liters of fluorescence dye were added after the well plates have been treated. Further, the cells were examined with fluorescent dyes under a fluorescence microscope [44].

2.8. Photocatalytic activities of methylene blue dye degradation

Photocatalytic activities of green synthesized Ai-FeO NPs were analyzed using methylene blue degradation in presence of sunlight radiations at different time intervals. As an inventory solution, methylene blue (1 mg) dye was dissolved in double distilled water (100 mL). 20 mg of green synthesized Ai-FeO NPs were distributed in 50 mL of methylene blue dye solution. A control was used without the inclusion of Ai-FeO NPs. Before exposing to irradiation, the reaction suspension was carefully mixed by using magnetic agitator for 30 min to confirm that the

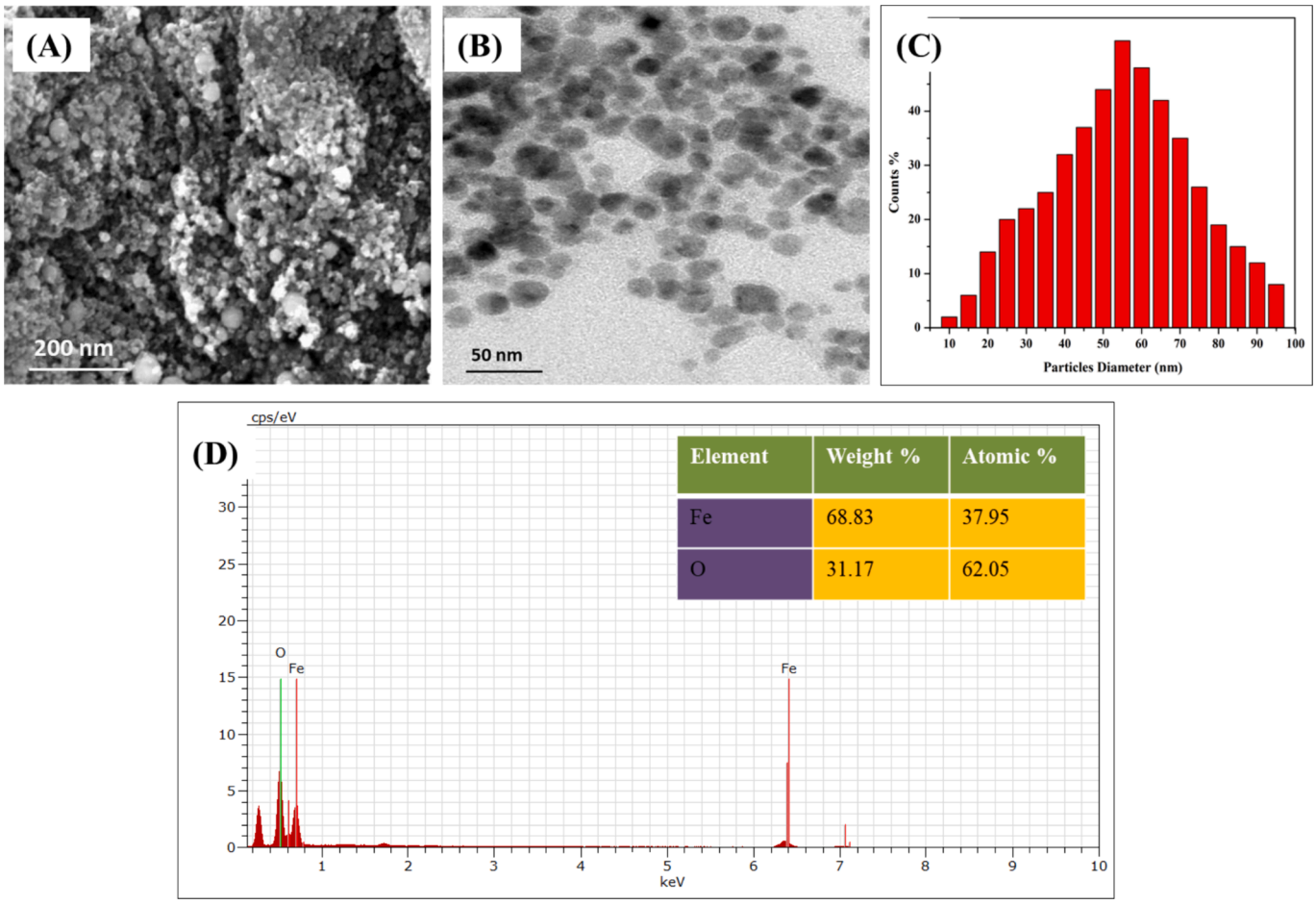

Fig. 2. (A) SEM image of *A.indicum*-synthesized FeO NPs (B) HR-TEM image of *A.indicum*-synthesized FeO NPs (C) Particle size distribution pattern of Ai-FeO NPs and (D) EDX analysis of *A.indicum*-synthesized FeO NPs.

working solution is homogeneous. The dispersion was then exposed to sunlight and monitored for different time intervals. Aliquots of 5 mL solutions were obtained and filtered at specific time intervals to examine the photocatalytic degradation of dye via UV spectra in the range 200–700 nm.

3. Statistical analysis

The ANOVA Tukey's HSD test was carried out using the IBM SPSS statistics software. Means were compared by the least significant difference (LSD) method at $p < 0.05$.

4. Results and discussion

4.1. 1. Green synthesis and characterization of Ai-FeO NPs

An environmentally friendly approach was used to synthesis FeO nanoparticles from *A. indicum* leaf extract. The green synthesized FeO NPs was preliminary confirmed by a distinctive transformation of the plant extract solution's color from yellow to a dark brown solution when the iron salt solution was introduced. *A. indicum* leaf extract contains active phytochemicals that reduce Fe ions to FeO NPs by the excitation of surface Plasmon resonances (SPR) on synthesized Ai-FeO NPs, resulting in Fe metal reduction [10,19]. Based on the spectra Fig. 1A, the peak surface plasmon resonance (SPR) bands at around 415 nm, which is in agreement with the previously reported SPR for FeO NPs using pomegranate seeds extract [18]. A similar study was conducted by Viju Kumar et al. (2018) [45] who measured the absorbance spectra of FeO NPs in the 330–400 nm range.

The crystalline nature of the synthesized Ai-FeO NPs was determined by XRD analysis. The peak positions with 2θ values corresponding to 30.3°, 35.62°, 43.56°, 54.2°, 57.7°, 63.6°, and 74.2° are associated with the indexed planes (200), (311), (400), (422), (511), (440), and (533), respectively (Fig. 1B). Undoubtedly, the strong and distinct peaks indicates that the Fe_2O_3 nanoparticles produced by the reduction process using *A. indicum* leaf extract were of crystalline nature. According to the database of the Joint Committee on Powder Diffraction Standards (JCPDS No. 00–003–0863), these peaks indicate that the synthesized Ai-FeO NPs are of crystalline structures in nature. The results are nearly identical to those reported by other research associated with iron oxide nanoparticles [31,46].

The biomolecules present in *A. indicum* plant extract induce the reduction of Fe to Ai-FeO NPs which was confirmed using FTIR measurements. Fig. 1 (C) of FTIR spectra shows peaks at 3428, 2922, 2852, 1630, 1601, 1383, 1112, 1036, 781, 619 and 534 cm^{-1}. The broad peak at 3428 cm^{-1} was attributed to the primary amine and amide (O—H stretching). The peaks at 2922 and 2852 cm^{-1}, corresponds to C—H stretching in alkanes and carboxylic acid O—H stretching. The presence of secondary amine, amide is indicated by the medium spectral peaks at 1630, 1601 cm^{-1}. It is worth noting that the Fe-O bonds of magnetite have a characteristic vibration between 619 and 500 cm^{-1}. Our findings are also in agreement with earlier reports that show the presence of FeO NPs in peak ranging from 400 to 624 cm^{-1} [47].

The shape and size of the green synthesized Ai-FeO NPs by *A. indicum* leaf extract was shown in Fig. 2A, B. TEM image shows an excellent distribution of spherical Ai-FeO NPs with no aggregation. Furthermore,

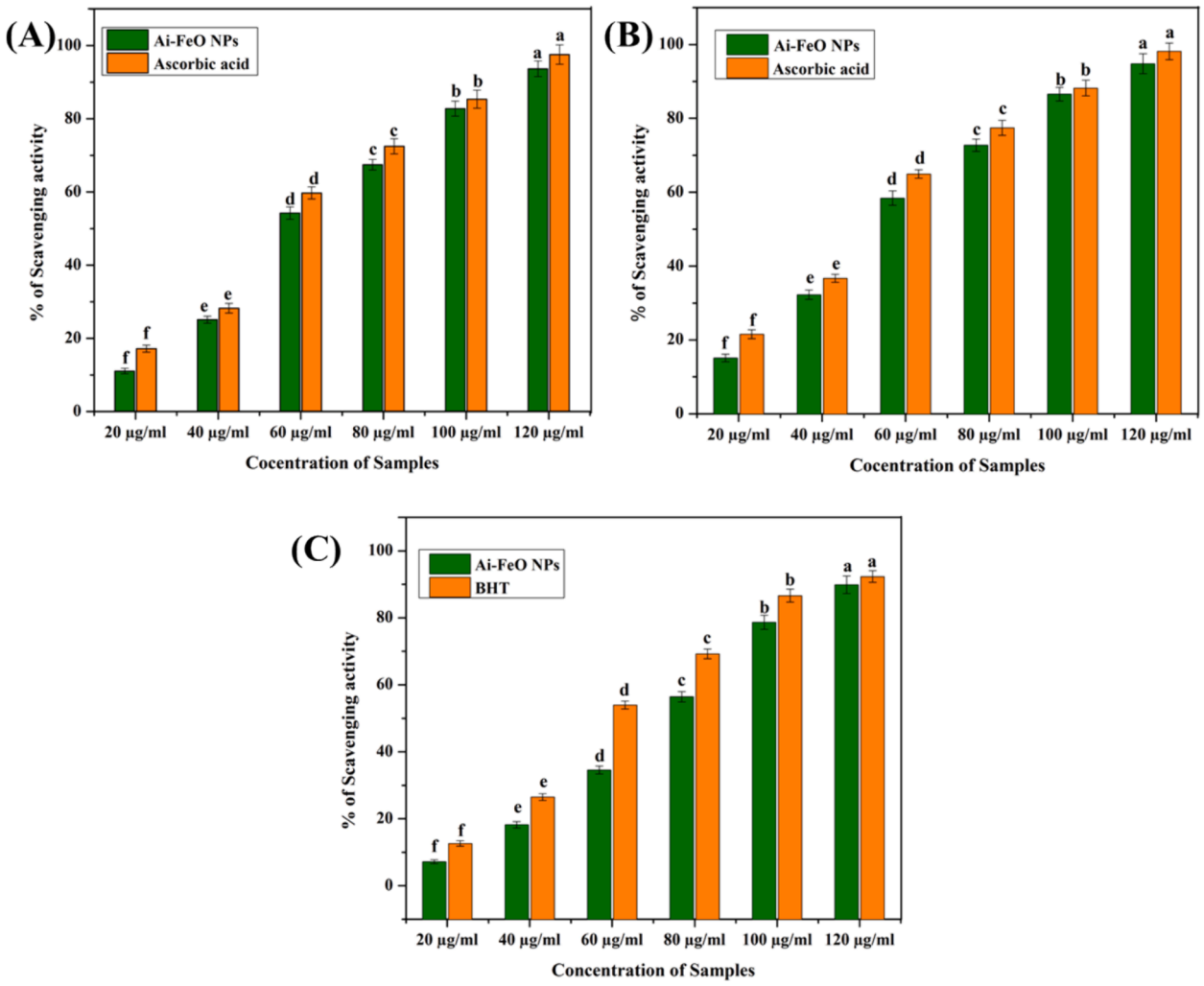

Fig. 3. Percentage of DPPH scavenging activity of Ascorbic acid and Ai-FeO NPs; (B) ABTS Radical scavenging activity of Ascorbic acid and Ai-FeO NPs; (C) Nitric oxide scavenging activity of BHT and Ai-FeO NPs. The data represents the mean values of three independent experiments and are presented as mean ± SD of the absorbance. Different letters indicated the significance differences (ANOVA followed by Tukey's HSD, α = 0.005).

Table 1
IC_{50} scavenging activity of green synthesized Ai-FeO NPs, Ascorbic acid.

Assays	IC_{50} value	
	Stranded	Ai-FeO NPs
DPPH	52.21 ± 1.22[a]	60.41 ± 1.68[a]
ABTS	47.27 ± 1.55[b]	56.62 ± 2.04[b]
NO	58.39 ± 1.46[c]	75.14 ± 2.63[c]

Values mean ± SD indicates the replicates of three experiments.
*Mean values within the column followed by the same ANOVA letter in superscript are significantly different at $P < 0.05$ level.

imaging examination revealed that the size of the synthesized Ai-FeO NPs ranged from 10 to 95 nm as indicated in Fig. 2C. Recently, *Hibiscus rosa sinensis flower* extract was used to create spherical FeO NPs with a particle size 55 nm [14]. EDX analysis was used to analyze the quantitative elemental mapping of green produced Ai-FeO NPs (Seen in Fig. 2D). The data analysis revealed that the synthesized Ai-FeO NPs contains Fe, O, with weight percentages of 68.83, and 31.17 %, respectively. EDX results reveal that FeO NPs was successfully synthesized from *A. indicum*. According to EDX analysis, Fe and O made up the majority of the elements in the nanostructure.

4.2. Radical scavenging activity of Ai-FeO NPs

The DPPH scavenging activity of the two samples (Ai-FeO NPs, Ascorbic acid) was conducted in triplicate. The DPPH free radical is considered to be a stable free radical that plays a critical role in the reduction of hydrogen or electrons from donors [48]. The Ai-FeO NPs ability to reduce DPPH was evaluated based on color change. The green synthesized Ai-FeO NPs demonstrated good scavenging performance but slightly low activity in comparison to the L-ascorbic acid. The percentage inhibition for different concentration (like 20, 40, 60, 80, 100 and 120 µg/ml) of Ai-FeO NPs and ascorbic acid samples was tested. Our results show a scavenging activity of 11.08 ± 0.75, 25.13 ± 0.98, 54.27 ± 1.68, 67.46 ± 1.44, 82.77 ± 2.06 and 93.61 ± 2.14 for Ai-FeO NPs. However, ascorbic acid was found to be 17.19 ± 0.94, 28.26 ± 1.32, 59.73 ± 1.65, 72.48 ± 2.07, 85.36 ± 2.47 and 97.55 ± 2.63 respectively which are seen in Fig. 3 (A). On the other hand, the IC_{50} values for DPPH scavenging activity for Ai-FeO NPs and L-ascorbic acid were determined from the plotted regression graph to be 60 µg/ml and 52 µg/ml, respectively, (Table 1). Comparably, Younas et al. [49] highlighted that *Ixora finlaysoniana* extract derived Fe-Cu bimetallic nanoparticles exhibited DPPH radical scavenging activity at concentrations of 200–600 ppm respectively.

As a result of their reducing power assay, they can donate an electron and can inhibit the oxidation of intermediates in the lipid peroxidation

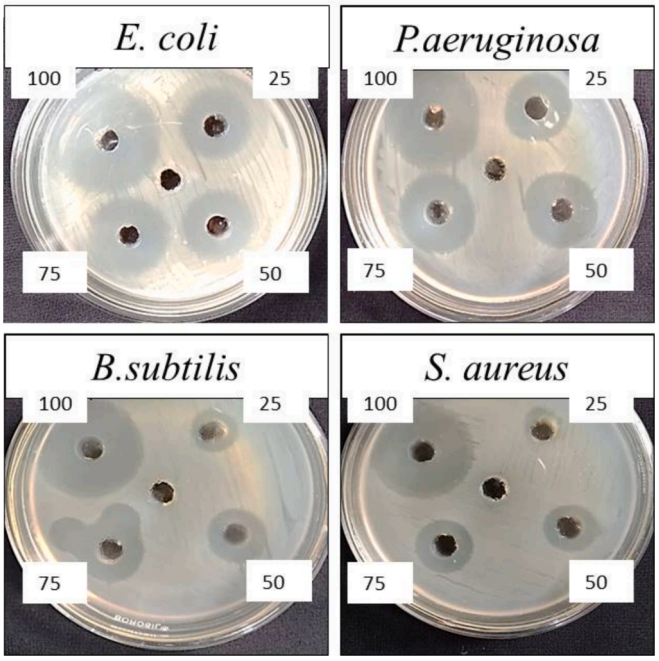

Fig. 4. Antibacterial activity *A.indicum* synthesized FeO NPs on *S. aureus*, *B. subtilis*, *E.coli,* and *P. aeruginosa.*

Table 2
Antimicrobial activity of green synthesized Ai-FeO NPs and *A. indicum* leaf extract.

Samples	Bacteria	Zone of inhibition (mm)			
		Concentration of samples			
		25 μg/ml	50 μg/ml	75 μg/ml	100 μg/ml
Ai-FeO NPs	*E. coli*	8.12 ± 0.72^{d}	11.31 ± 0.93^{c}	16.68 ± 0.98^{b}	19.25 ± 1.08^{a}
	P. aeruginosa	5.48 ± 0.67^{d}	8.62 ± 0.47^{c}	11.16 ± 0.85^{b}	16.56 ± 0.64^{a}
	S. aureus	3.51 ± 0.72^{d}	6.92 ± 0.21^{c}	8.21 ± 0.66^{b}	12.63 ± 1.07^{a}
	B.subtilis	4.68 ± 0.56 ^{d}	7.24 ± 0.63^{c}	9.32 ± 0.24^{b}	14.88 ± 1.01 ^{a}
***A. indicum* leaf extract**	*E. coli*	6.36 ± 0.82^{d}	10.24 ± 0.55^{c}	14.39 ± 0.79^{b}	17.42 ± 1.07^{a}
	P. aeruginosa	5.14 ± 0.47^{d}	7.43 ± 0.26^{c}	9.66 ± 0.36^{b}	13.15 ± 0.88^{a}
	S. aureus	2.07 ± 0.13 ^{d}	4.03 ± 0.13^{c}	5.96 ± 0.47^{b}	8.63 ± 0.57 ^{a}
	B.subtilis	3.98 ± 0.26^{d}	5.12 ± 0.67^{c}	7.06 ± 0.68^{b}	12.64 ± 0.69^{a}

Values mean ± SD indicates the replicates of three experiments.
*Mean values within the column followed by the same ANOVA letter in superscript are significantly different at $P < 0.05$ level.

process. They constitute both primary and secondary antioxidants [42]. At higher concentration (120 μg/mL) of L-ascorbic acid displayed 97.15 ± 2.25 % superior reducing power activity flowed by Ai-FeO NPs 94.81 ± 2.70 %, which are summarized in Fig. 3B. The IC_{50} values of reducing power activity for Ai-FeO NPs and L-ascorbic acid were determined from the plotted regression graph is found to be 56 μg/ml and 47 μg/ml, respectively (Table 1).

Nitric oxide (NO) is a bioregulatory molecule that is vital in the neurological, immunological, and cardiovascular systems. Fig. 3C revealed higher concentration (120 μg/mL) of BHT displayed 92.32 ± 1.74 % superior NO scavenging activity flowed by Ai-FeO NPs 89.92 ± 2.62 %. At lower concentration (20 μg/mL) of BHT displayed 12.63 ± 0.81 % superior NO scavenging activity flowed by Ai-FeO NPs 7.16 ± 0.62 %. In addition, IC_{50} values for NO scavenging activity for Ai-FeO NPs and BHT were determined from the plotted regression graph is found to be 75 μg/ml and 58 μg/ml, respectively as indicated in Table 1. Phytochemicals in the extract were responsible for the reducing power activity [50]. The results obtained in this study were similar to those of

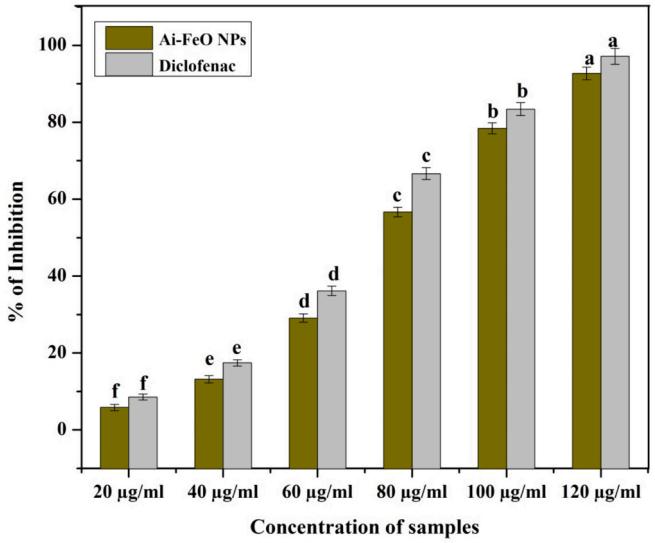

Fig. 5. (A) Anti inflammation of green synthesized Ai-FeO NPs and diclofenac against albumin, the data represents the mean values of three independent experiments and are presented as mean ± SD of the absorbance. Different letters indicated the significance differences (ANOVA followed by Tukey's HSD, α = 0.005).

Table 3
Cytotoxic activity of Cisplatin and Ai-FeO NPs (μg/ml).

S. No	Samples	MDA-MB-231(IC_{50})
1	Cisplatin	85.32 ± 2.72
2	Ai-FeO NPs	66.55 ± 1.46

IC_{50} – Values of respective samples at 48 h.

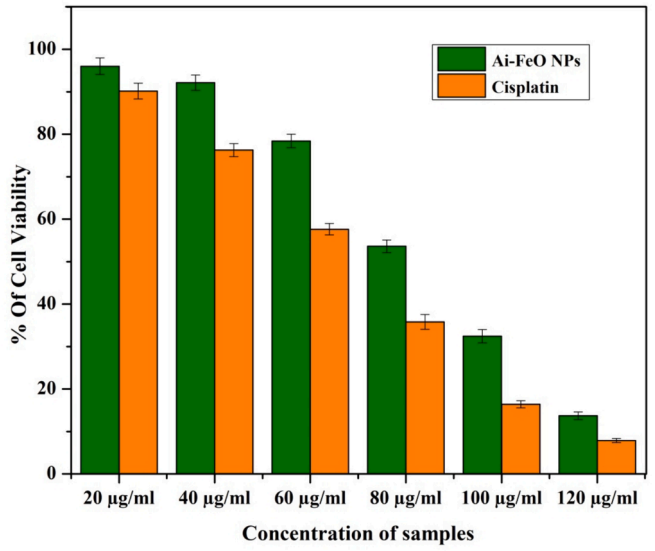

Fig. 6. Cytotoxic potential of *A.indicum* synthesized Ai-FeO NPs and Cisplatin against MDA-MB-231 cells. The data represents the mean values of three independent experiments and are presented as mean ± SD of the absorbance.

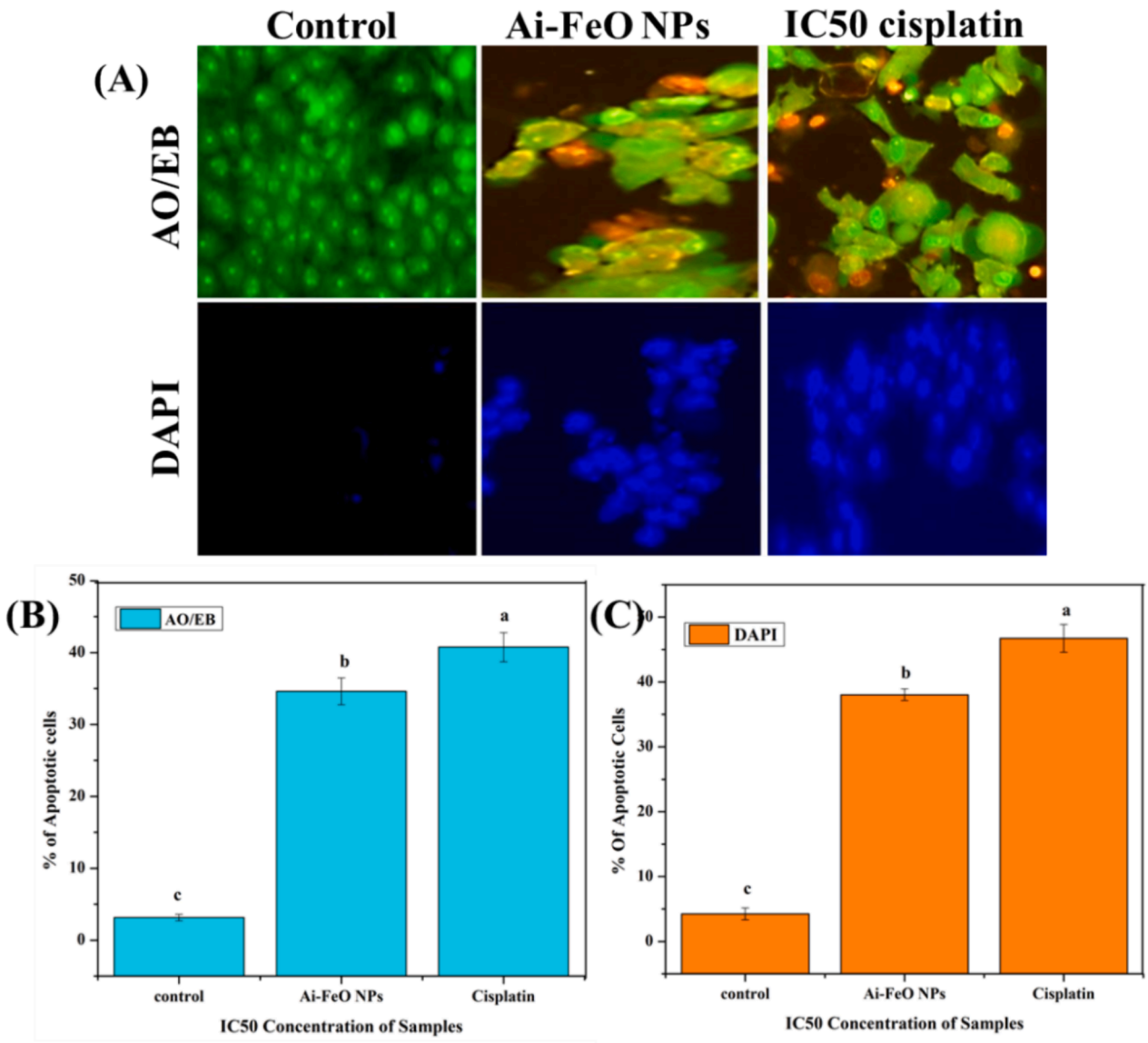

Fig. 7. Bright field and fluorescence microscopy of MDA-MB-231 cells treated with IC_{50} concentrations of Ai-FeO nanoparticles and cisplatin; (A) Fluorescence microscopy of AO/EtBr-stained control cells Ai-FeO NPs and Cisplatin treated cells (live cells in green color and dead cell in orange color, in the treated sample. DAPI nuclear staining of control cells and Ai-FeO NPs Cisplatin treated cells exhibited a condensed form of nuclear materials in apoptotic cells. (B, C) Histogram representation of the percentage of total observed apoptotic cells against the IC_{50} concentration of Ai-FeO NPs and Cisplatin formulated on selected MDA-MB-231 cells after 48 h. The data represents the mean values of three independent experiments and are presented as mean ± SD of the absorbance. Different letters indicated the significance differences (ANOVA followed by Tukey's HSD, $\alpha = 0.005$).

Dipankar and Murugan [51] reported earlier.

4.3. Antibacterial (zone of inhibition) activity of Ai-FeO NPs

The agar well diffusion method was used to evaluate the antibacterial activity of the synthesized Ai-FeO NPs and *A. indicum* leaf extract (Fig. 4). The zone of inhibition around the well containing different concentrations of samples was examined. The results show that the highest dose of Ai-FeO NPs was effective against both Gram-positive (*S. aureus, B. subtilis*) and Gram-negative bacteria (*E. coli, P. aeruginosa*), which are represented in Table 2. The data reported in Table 2 indicated that aqueous extract of *A. indicum* leaf extract had very low inhibitory effects on all the tested strains. The higher concentration of Ai-FeO NPs (100 μg/mL) displayed DIZs for *E. coli, P. aeruginosa*, *S. aureus,* and *B. subtilis* are 19.25 ± 1.08 mm, 16.56 ± 0.6 mm, 12.63 ± 1.07 mm and 14.88 ± 1.01 respectively, which are shown in Fig. 4. At lower concentration of Ai- FeO NPs showed DIZs for *E. coli, P. aeruginosa*, and *S. aureus, B. subtilis* are 8.12 ± 0.72 mm, 5.48 ± 0.67 mm, 3.51 ± 0.72 and 4.68 ± 0.56. In general, iron oxide nanoparticles shown antibacterial activity due to their ability of reactive oxygen species (ROS) production, cell membrane breakage and DNA damage, which leads to the cell death [23,52]. It was found that green synthesized FeO nanoparticles were more effective against Gram-negative bacteria than Gram-positive bacteria. Similarly, the green synthesized Ag doped CeO_2 showed enhanced antibacterial properties on *E. coli* and *S. aureus* [53]. The structural and compositional differences in the membranes of these two types of bacteria may lead to the difference in their activity [54,55]. These green synthesized FeO NPs would find it harder to permeate Gram-positive bacteria thicker peptidoglycan cell walls than Gram-negative bacteria, as there would be less of an antibacterial reaction [40].

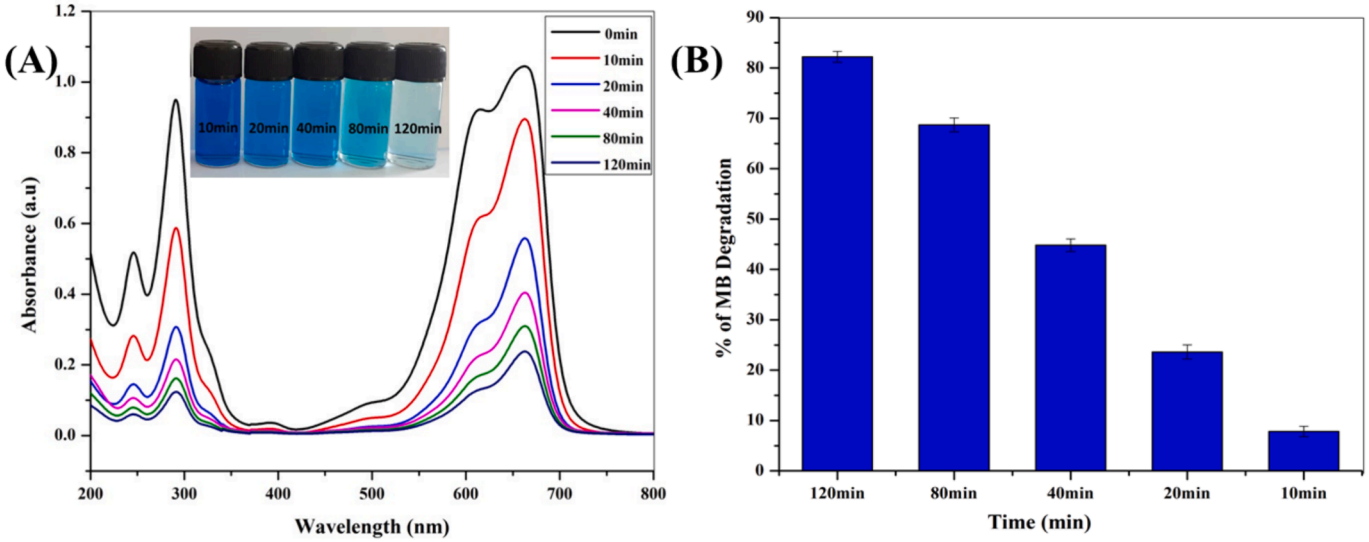

Fig. 8. Photocatalytic activity of *A.indicum* synthesized Ai-FeO nanoparticles.

4.4. *In-vitro anti-inflammatory activity*

The immune system of the body automatically produces inflammation in reaction to a variety of pathogens, irritants, damaged cells, and damaging stimuli. Protein breakdown can also result in inflammation. In this work, we have evaluated the anti-inflammatory potential of Ai-FeO NPs using Albumin denaturation assays. Due to the external stress, proteins get denaturized and lose their biological functions as well as their secondary and tertiary structures. Fig. 5 revealed the green synthesized Ai-FeO NPs had a dose dependant anti-inflammatory activity. The activity of Ai-FeO NPs on Bovine Serum Albumin was increased and directly proportional to the concentration (20 μg/mL–5.82 %; 40 μg/mL–13.16 %; 60 μg/mL–29.08 %, 80 μg/mL–56.66, 100 μg/mL-78.42 and 120 μg/mL–92.71 %). Furthermore, diclofenac revealed a minimum inhibition of 8.54 % at a concentration of 20 μg/mL and maximum inhibition of 97.15 % at a 120 μg/mL concentration as shown in Fig. 5. Our results are well matched with Alahmdi et al. [19] revealed that zinc oxide nanoparticles from *Clitoria ternatea* flower extract exhibited significant anti-inflammatory activity in a dose dependent manner,

4.5. *Cytotoxic effect of Ai-FeO NPs using MDA-MB-231 cell line*

The MTT assay is used to evaluate cellular metabolic activity which is the predictor of cell viability, proliferation, and cytotoxicity of a molecule. This colorimetric assay is principally based on the conversion of a yellow tetrazolium salt (three-four, five-dimethylthiazol-2-yl)-2, 5-diphenyl tetrazolium bromide or MTT) to red formazan crystals through metabolically active cells. The MTT is transformed to formazan by NADPH dependent oxidoreductase enzymes in live cells [56]. Fig. 6 demonstrates the different concentration of Ai-FeO nanoparticles in solutions at concentrations of 10 μg/ml, 20 μg/ml, 40 μg/ml, 60 μg/ml, 80 μg/ml and 100 μg/ml, giving viability reports of 96 %, 92 %, 78 %, 53 %, 32 % and 13 %. On the other hand, commercial drug in solutions at different concentrations like 10 μg/ml, 20 μg/ml, 40 μg/ml, 60 μg/ml, 80 μg/ml and 100 μg/ml, giving viability reports of 90 %, 76 %, 57 %, 35 %, 16 % and 7 %. From these results, we conclude that the green synthesized FeO NPs had a great cytotoxic effect against MDA-MB-231 cells, but slightly lower cytotoxic compared to commercial drug. The IC_{50} values of MDA-MB-231 in the presence of Ai-FeO NPs and cisplatin were calculated to be 85 and 66 μg/ml, respectively (Table 3). Nanoparticles can pass across the cellular membrane and influence the mRNA expression of suppression genes, causing the production of reactive oxygen species (ROS) in cells to increase [57]. Unexpectedly, more external ROS are produced by metal oxide nanoparticles, despite the fact that this is one of the signs of a severe cytotoxicity effect [58].

4.5.1. *Dual staining (AO/EB) and DAPI analysis of apoptosis*

The ability of Ai-FeO NPs (IC_{50}) to destabilise cell membranes was assessed by using the AO/EB assay in comparison with the controls. The results showed that the early apoptosis was increased, and number of viable cells decreased after the treatment. AO and EB dual staining was employed to search for various apoptotic indicators in nucleate alternations (Fig. 7a**)**. The percentage of cellular damage was reported to be 40.76 ± 2.03 and 34.62 ± 1.85, in treated and control cells respectively. Apoptosis-induced early cell shrinkages, DNA fragmentation, *peri*-nuclear condensed chromatin, and late apoptosis-induced fragmented chromatin and cell nuclei disintegration were clearly visible in green synthesized Ai-FeO NPs treated cells. The DAPI stained negative control and Ai-FeO NPs treated cells (Conc. same as IC50 value) and positive control (cisplatin) treated MDA-MB-231 were also analysed there was a significant number of apoptotic nuclei in Ai-FeO NPs treated cells (Fig. 7**b**). The nuclear condensation rate due to Apoptosis was found to be 38.03 ± 1.08 and 46.72 ± 2.14 respectively (**figure c**).

4.6. *Photocatalytic activity of Ai-FeO NPs*

The pharmaceutical, textile, and dyeing sectors essentially employ a lethal synthetic colour known as methylene blue. Methylene blue has a potential to upset the balance of aquatic and biological systems [59]. In this work, we have carried out the photocatalytic activity of green synthesized Ai-FeO NPs against methylene blue (MB). The following conditions were used to study the degradation of MB: The reaction mixture of 50 ml of MB and 25 mg of Ai-FeO nanoparticles were exposed to sunlight for various time intervals. The MB was gradually photo degraded during this process, and the colour of the solution changed from an initial deep blue to nearly translucent, the absorbance intensity gradually diminishes with longer contact durations, that indicates the photocatalytic degradation (Fig. 8). In case of control where Ai-FeO NPs was absent methylene blue could not degrade under the irradiation of sun light. The percentage of MB that was degraded at different time intervals (120 min, 80 min, 40 min, 20 min, and 10 min) and their percentages of removal 82.24, 68.42, 44.68, 23.62, and 7.83 %, respectively are shown in Fig. 6b. Similarly, *Gazania rigens* synthesized Cu-Ni bimetallic nanoparticles efficiently degrade the methylene blue under UV light irradiation after 19 mins treatment with a rate constant of 0.2505 min^{-1} [60]. Our result indicated that the presence of green

synthesised Ai-FeO NPs was causing the methylene blue degradation in time-dependent manner.

5. Conclusion

Recently, plant extracts have been employed in the development of environmentally friendly nanoparticles via green synthesis approach for several therapeutic purposes as they possess low toxicity and are cost-effective. Nowadays, nanoparticles are used in many aspects of medicinal research such as antimicrobial, cancer research, drug delivery etc. Keeping this in mind we focused our research to green synthesize FeO nanoparticles using leaf extracts of *A.indicum.*Further, the physical and chemical properties of obtained Ai-FeO NPs were thoroughly investigated by UV–vis spectroscopy, XRD, FTIR, SEM, HR-TEM, and EDAX analysis. Furthermore, our results demonstrated that the green synthesized Ai-FeO NPs using *A. indicum* displayed appreciable biomedical properties, including antimicrobial, antioxidant, anti-inflammatory, and anti-apoptotic activities. Overall, according to our study the *A. indicum*-synthesized Ai-FeO NPs can be a potential candidate for variety of therapeutic drugs especially as biosafe and cost-effective antioxidant, antibacterial, and a significant anti-breast cancer drug.

Funding

The authors state no funding involved.

CRediT authorship contribution statement

Chellasamy Panneerselvam: . **Mohammed Ali Alshehri:** Data curation. **Ahmed Saif:** . **Uzma Faridi:** Writing – original draft, Methodology. **Syed Khasim:** Writing – original draft, Methodology. **Zuhair M Mohammedsaleh:** Data curation. **Humaira Parveen:** Writing – original draft. **Noha Omer:** Writing – review & editing, Data curation. **Abdulrahman Alasmari:** Data curation. **Sayeed Mukhtar:** Writing – review & editing, Writing – original draft. **Hatem A. Al-Aoh:** Conceptualization.

Declaration of competing interest

The authors declare that they have no known competing financial interests or personal relationships that could have appeared to influence the work reported in this paper.

Data availability

Data will be made available on request.

References

[1] F. Bray, J. Ferlay, I. Soerjomataram, R.L. Siegel, L.A. Torre, A. Jemal, Global cancer statistics 2018: GLOBOCAN estimates of incidence and mortality worldwide for 36 cancers in 185 countries, CA Cancer J. Clin. 68 (6) (2018) 394–424.

[2] C. Panneerselvam, A.I. Alalawy, K. Albalawi, H.S. Al-Shehri, H. Parveen, H.A. Al-Aoh, N.S. Bedowr, F.J. Mujammami, M. Nusari, S. Khateeb, Anticancer activity of bioactive compound chavicol as potential toxic against human cancer A549 cells, J. Drug. Deliv. Sci. Technol. 73 (2022) 103442, https://doi.org/10.1016/j.jddst.2022.103442.

[3] C. Dunnill, T. Patton, J. Brennan, J. Barrett, M. Dryden, J. Cooke, N. T. Georgopoulos, Reactive oxygen species (ROS) and wound healing: the functional role of ROS and emerging ROS-modulating technologies for augmentation of the healing process, Int. Wound J. 14 (1) (2017) 89–96, https://doi.org/10.1111/iwj.12557.

[4] L. Corti, Nonpharmaceutical approaches to pain management, Top. Companion. Anim. Med. 29 (1) (2014) 24–28.

[5] T.M. Joseph, D. Kar Mahapatra, A. Esmaeili, L. Piszczyk, M.S. Hasanin, M. Kattali, J. Haponiuk, S. Thomas, Nanoparticles: taking a unique position in medicine, Nanomaterials 13 (3) (2023) 574, https://doi.org/10.3390/nano13030574.

[6] J.K. Patra, K.H. Baek, Green nanobiotechnology: factors affecting synthesis and characterization techniques, J. Nanomaterials. 2015 (2014) 219.

[7] Z.U.K. Khan, N.S. Gul, S. Sabahat, J. Sun, K. Tahir, N.S. Shah, N. Muhammad, A. Rahim, M. Imran, J. Iqbal, T.M. Khan, S. Khasim, U. Farooq, J. Wu, Removal of organic pollutants through hydroxyl radical-based advanced oxidation processes, Ecotoxicol. Environ. Saf. 267 (2023) 115564.

[8] C. Pandit, A. Roy, S. Ghotekar, A. Khusro, M.N. Islam, T.B. Emran, S.E. Lam, M. U. Khandaker, D.A. Bradley, Biological agents for synthesis of nanoparticles and their applications, J. King Saud Uni. Sci. 34 (3) (2022) 101869, https://doi.org/10.1016/j.jksus.2022.101869.

[9] S. Vijayaram, H. Razafindralambo, Y.Z. Sun, S. Vasantharaj, H. Ghafarifarsani, S. H. Hoseinifar, M. Raeeszadeh, Applications of green synthesized metal nanoparticles—a review, Biol. Trace Elem. Res. 202 (1) (2024) 360–386.

[10] C. Panneerselvam, K. Murugan, M. Roni, A.T. Aziz, U. Suresh, R. Rajaganesh, G. Benelli, Fern-synthesized nanoparticles in the fight against malaria: LC/MS analysis of *Pteridium aquilinum* leaf extract and biosynthesis of silver nanoparticles with high mosquitocidal and antiplasmodial activity, Parasitol. Res. 115 (2016) 997–1013.

[11] S.A. Al-Ghamdi, T.A. Alkathiri, A.E. Alfarraj, O.M. Alatawi, A.S. Alkathiri, C. Panneerselvam, S. Vanaraj, A.A.A. Darwish, T.A. Hamdalla, A. Pasha, S. Khasim, Green synthesis and characterization of zinc oxide nanoparticles using *Camellia sinensis* tea leaf extract and their antioxidant, anti–bactericidal and anticancer efficacy, Res. Chem. Intermed. 48 (2022) 4769–4783.

[12] J. Virkutyte, R.S. Vara, Environmentally friendly preparation of metal nanoparticles, Sustainable Preparation of Metal Nanoparticles: Methods and Applications, Royal Soc. Chem. London, UK (2013) 7–33, https://doi.org/10.1039/9781849735469-00007.

[13] D. Bhattacharya, R.K. Gupta, Nanotechnology and potential of microorganisms, Crit. Rev. Biotechnol 25 (4) (2005) 199–204, https://doi.org/10.1080/07388550500361994.

[14] F. Buarki, H. AbuHassan, F. Al Hannan, F.Z. Henari, Green synthesis of iron oxide nanoparticles using *Hibiscus rosa sinensis* flowers and their antibacterial activity, J. Nanotechnol. (2022), https://doi.org/10.1155/2022/5474645.

[15] T. Shahwan, S.A. Sirriah, M. Nairat, E. Boyacı, A.E. Eroğlu, T.B. Scott, K.R. Hallam, Green synthesis of iron nanoparticles and their application as a Fenton-like catalyst for the degradation of aqueous cationic and anionic dyes, Chem. Eng. J. 172 (1) (2011) 258–266, https://doi.org/10.1016/j.cej.2011.05.103.

[16] E.F. El-Belely, M.M. Farag, H.A. Said, A.S. Amin, E. Azab, A.A. Gobouri, A. Fouda, Green synthesis of zinc oxide nanoparticles (ZnO-NPs) using *Arthrospira platensis* (Class: Cyanophyceae) and evaluation of their biomedical activities, Nanomaterials 11 (1) (2021) 95, https://doi.org/10.3390/nano11010095.

[17] S. Meneceur, H. Hemmami, A. Bouafia, S.E. Laouini, M.L. Tedjani, D. Berra, M. S. Mahboub, Photocatalytic activity of iron oxide nanoparticles synthesized by different plant extracts for the degradation of diazo dyes Evans blue and Congo red, Biomass Conv. Bioref. 14 (2024) 5357–5372, https://doi.org/10.1007/s13399-022-02734-4.

[18] T.S. Aragaw, F.M. Bogale, B.A. Aragaw, Iron-based nanoparticles in wastewater treatment: A review on synthesis methods, applications, and removal mechanisms, J. Saudi Chem. Soc. 25 (2021) 101280, https://doi.org/10.1016/j.jscs.2021.101280.

[19] M.I. Alahmdi, S. Khasim, S. Vanaraj, C. Panneerselvam, M.A.A. Mahmoud, S. Mukhtar, M.A. Alsharif, N.S. Zidan, N.E. Abo-Dya, O.F. Aldosari, Green nanoarchitectonics of ZnO nanoparticles from *Clitoria ternatea* flower extract for in vitro anticancer and antibacterial activity: Inhibits MCF–7 cell proliferation via intrinsic apoptotic pathway, J. Inorg. Organomet. Polym. Mater 32 (2022) 2146–2159, https://doi.org/10.1007/s10904-022-02263-7.

[20] M.S.H. Bhuiyan, M.Y. Miah, S.C. Paul, T.D. Aka, O. Saha, M.M. Rahaman, M. Ashaduzzaman, Green synthesis of iron oxide nanoparticle using *Carica papaya* leaf extract: application for photocatalytic degradation of remazol yellow RR dye and antibacterial activity, Heliyon 6 (8) (2020) e04603.

[21] E. Rostamizadeh, A. Iranbakhsh, A. Majd, S. Arbabian, I. Mehregan, Green synthesis of Fe_2O_3 nanoparticles using fruit extract of *Cornus mas* L. and its growth-promoting roles in Barley, J. Nanostruct. Chem. 10 (2020) 125–130, https://doi.org/10.1007/s40097-020-00335-z.

[22] A. Shah, M.A. Dobrovolskaia, Immunological effects of iron oxide nanoparticles and iron-based complex drug formulations: Therapeutic benefits, toxicity, mechanistic insights, and translational considerations, Nanomedicine 14 (3) (2018) 977–990, https://doi.org/10.1016/j.nano.2018.01.014.

[23] B.A. Abbasi, J. Iqbal, T. Mahmood, A. Qyyum, S. Kanwal, Biofabrication of iron oxide nanoparticles by leaf extract of *Rhamnus virgata*: Characterization and evaluation of cytotoxic, antimicrobial and antioxidant potentials, Appl. Organomet. Chem. 33 (7) (2019) e4947.

[24] S. Vasantharaj, S. Sathiyavimal, P. Senthilkumar, F. LewisOscar, A. Pugazhendhi, Biosynthesis of iron oxide nanoparticles using leaf extract of *Ruellia tuberosa*: antimicrobial properties and their applications in photocatalytic degradation, J. Photochem. Photobiol. b: Biol 192 (2019) 74–82, https://doi.org/10.1016/j.jphotobiol.2018.12.025.

[25] B.A. Abbasi, J. Iqbal, S.A. Zahra, A. Shahbaz, S. Kanwal, A. Rabbani, T. Mahmood, Bioinspired synthesis and activity characterization of iron oxide nanoparticles made using *Rhamnus triquetra* leaf extract, Mater. Res. Express 6 (12) (2020), https://doi.org/10.1088/2053-1591/ab664d, 1250e7.

[26] H.S. Devi, M.A. Boda, M. A. Shah, S. Parveen, A. H. Wani, Green synthesis of iron oxide nanoparticles using *Platanus orientalis* leaf extract for antifungal activity, Green Process. Synth, 8(1), 2-19, 38-45. 10.1515/gps-2017-0145.

[27] M.A. Shabbir, M. Naveed, S.U. Rahman, N.U. Ain, T. Aziz, M. Alharbi, A. Alsahammari, A.F. Alasmari, Synthesis of iron oxide nanoparticles from *Madhuca indica* plant extract and assessment of their cytotoxic, antioxidant, anti-inflammatory, and anti-diabetic properties via different nanoinformatics approaches, ACS Omega 8 (37) (2023) 33358–33366, https://doi.org/10.1021/acsomega.3c02744.

[28] S. Bishnoi, A. Kumar, R. Selvaraj, Facile synthesis of magnetic iron oxide nanoparticles using inedible *Cynometra ramiflora* fruit extract waste and their photocatalytic degradation of methylene blue dye, Mater. Res. Bull. 97 (2018) 121–127, https://doi.org/10.1016/j.materresbull.2017.08.040.

[29] N. Bibi, S. Nazar, M. Ata, A. Sultan, A. Ali, K. Abbas, S. Jilani, F.M. Kamal, M Iftikhar Sarim, F. Jalal Khan, M. Iqbal, Green synthesis of iron oxide nanoparticles using pomegranate seed extract and photocatalytic activity evaluation for the degradation of textile dye, J. Mat. Res. Technol. 8 (6) (2019) 6115–6124, https://doi.org/10.1016/j.jmrt.2019.10.006.

[30] H. Muthukumar, S.N. Mohammed, N. Chandrasekaran, A.D. Sekar, A. Pugazhendhi, M. Matheswaran, Effect of iron doped Zinc oxide nanoparticles coating in the anode on current generation in microbial electrochemical cells, Int. J. Hydrogen Energy. 44 (4) (2019) 2407–2416, https://doi.org/10.1016/j.ijhydene.2018.06.046.

[31] I. Bibi, N. Nazar, S. Ata, M. Sultan, A. Ali, A. Abbas, M. Iqbal, Green synthesis of iron oxide nanoparticles using pomegranate seeds extract and photocatalytic activity evaluation for the degradation of textile dye, J. Mat. Res. Technol 8 (6) (2019) 6115–6124, https://doi.org/10.1016/j.jmrt.2019.10.006.

[32] S.N. Suresh, P. Sagadevan, S.R. Kumar, V. Rajeshwari, Phytochemical analysis and antimicrobial potential of *Abutilon indicum* (Malvaceae), Int. J. Pharm. Res. Dev. 4 (2) (2012) 132–134.

[33] R. Mata, J.R. Nakkala, S.R. Sadras, Biogenic silver nanoparticles from *Abutilon indicum*: Their antioxidant, antibacterial and cytotoxic effects in vitro, ColloidsSurf. B: Biointerfaces 128 (2015) 276–286, https://doi.org/10.1016/j.colsurfb.2015.01.052.

[34] S. Umavathi, M. Subash, K. Gopinath, S. Alarifi, M. Nicoletti, M. Govindarajan, Facile synthesis and characterization of ZnO nanoparticles using *Abutilon indicum* leaf extract: An eco-friendly nano-drug on human microbial pathogens, J. Drug Deliv. Sci. Technol. 66 (2021) 102917, https://doi.org/10.1016/j.jddst.2021.102917.

[35] F. Ijaz, S. Shahid, S.A. Khan, W. Ahmad, S. Zaman, Green synthesis of copper oxide nanoparticles using *Abutilon indicum* leaf extract: Antimicrobial, antioxidant, and photocatalytic dye degradation activitie, Trop. J. Pharm. Res. 16 (4) (2017) 743–753, https://doi.org/10.4314/tjpr.v16i4.2.

[36] S.A. Khan, S. Shahid, B. Shahid, U. Fatima, S. Abbasi, Green synthesis of MnO nanoparticles using *Abutilon indicum* leaf extract for biological, photocatalytic, and adsorption activities, Biomolecules 10 (5) (2020) 785, 10.3390%2Fbiom10050785.

[37] S.A. Khan, S. Shahid, A. Ayaz, J. Alkahtani, M.S. Elshikh, T. Riaz, Phytomolecules-coated NiO nanoparticles synthesis using *Abutilon indicum* leaf extract: antioxidant, antibacterial, and anticancer activities, Int. J. Nanomedicine 16 (2021) 1757, 10.2147%2FIJN.S294012.

[38] J. Venkatesan, S.K. Kim, M.S. Shim, Antimicrobial, antioxidant, and anticancer activities of biosynthesized silver nanoparticles using marine algae *Ecklonia cava*, Nanomaterials 6 (12) (2016) 235, 10.3390%2Fnano6120235.

[39] A. Vinothkanna, K. Mathivanan, S. Ananth, Y. Ma, S. Sekar, Biosynthesis of copper oxide nanoparticles using *Rubia cordifolia* bark extract: characterization, antibacterial, antioxidant, larvicidal and photocatalytic activities, Env. Sci. Pollut. Res. 30 (2022) 42563–42574, https://doi.org/10.1007/s11356-022-18996-4.

[40] D.B. Manikandan, A. Sridhar, R.K. Sekar, B. Perumalsamy, S. Veeran, M. Arumugam, T. Ramasamy, Green fabrication, characterization of silver nanoparticles using aqueous leaf extract of *Ocimum americanum* (Hoary Basil) and investigation of its in vitro antibacterial, antioxidant, anticancer and photocatalytic reduction, J. Env Chem. Eng 9 (1) (2021) 104845, https://doi.org/10.1016/j.jece.2020.104845.

[41] S. Vanaraj, B.B. Keerthana, K. Preethi, Biosynthesis, characterization of silver nanoparticles using quercetin from *Clitoria ternatea* L to enhance toxicity against bacterial biofilm, J. Inorg. Organomet. Polym. Mater. 27 (5) (2017) 1412–1422. https://link.springer.com/article/10.1007/s10904-017-0595-8.

[42] G. Rajakumar, M. Thiruvengadam, G. Mydhili, T. Gomathi, I. Chung, Green approach for synthesis of zinc oxide nanoparticles from *Andrographis paniculata* leaf extract and evaluation of their antioxidant, antidiabetic, and anti-inflammatory activities, Bioprocess Biosyst Eng. 41 (1) (2018) 21–30, https://doi.org/10.1007/s00449-017-1840-9.

[43] R. Vivek, R. Thangam, K. Muthuchelian, P. Gunasekaran, K. Kaveri, S. Kannan, Green biosynthesis of silver nanoparticles from *Annona squamosa* leaf extract and its in vitro cytotoxic effect on MCF-7 cells, Process Biochem 47 (12) (2012) 2405–2410, https://doi.org/10.1016/j.procbio.2012.09.025.

[44] K. Murugan, D. Dinesh, K. Kavithaa, M. Paulpandi, T. Ponraj, M.S. Alsalhi, G. Benelli, et al., Hydrothermal synthesis of titanium dioxide nanoparticles: mosquitocidal potential and anticancer activity on human breast cancer cells (MCF-7), Parasitol. Res. 115 (3) (2016) 1085–1096, https://doi.org/10.1007/s00436-015-4838-8.

[45] V.G. Viju Kumar,A.A. Prem,Green synthesis and characterization of iron oxide nanoparticles using *Phyllanthus niruri* extract. Oriental J. Chem. 34(5), 2583-2589, https://doi.org/10.13005/ojc/340547.

[46] Y.P. Yew, K. Shameli, M. Miyake, N. Kuwano, N.B. Ahmad Khairudin, S. E. Mohamad, K.X. Lee, Green synthesis of magnetite (Fe_3O_4) nanoparticles using seaweed (Kappaphycus alvarezii) extract, Nanoscale Res. Lett. 11 (1) (2016) 276, https://doi.org/10.1186/s11671-016-1498-2.

[47] C.A. Silva, R.L. Silva, A.T.D. Figueiredo, V.N. Alves, Magnetic solid-phase microextraction for lead detection in aqueous samples using magnetite nanoparticles, J. Braz. Chem. Soc. 31 (1) (2020) 109–115, https://doi.org/10.21577/0103-5053.20190134.

[48] M. Govindappa, B. Hemashekhar, M.K. Arthikala, V.R. Rai, Y.L. Ramachandra, Characterization, antibacterial, antioxidant, antidiabetic, anti-inflammatory and antityrosinase activity of green synthesized silver nanoparticles using *Calophyllum tomentosum* leaves extract, Results. Phys. 9 (2018) 400–408, https://doi.org/10.1016/j.rinp.2018.02.049.

[49] U. Younas, S.T. Hassan, F. Ali, F. Hassan, Z. Saeed, M. Pervaiz, S. Khan, F.T. Jannat, S. Bibi, A. Sadiqa, et al., Radical scavenging and catalytic activity of Fe-Cu bimetallic nanoparticles synthesized from *Ixora finlaysoniana* extract, Coatings 11 (7) (2021) 813, https://doi.org/10.3390/coatings11070813.

[50] Y.L. Lin, I.M. Juan, Y.L. Chen, Y.C. Liang, J.K. Lin, Composition of polyphenols in fresh tea leaves and associations of their oxygen-radical-absorbing capacity with antiproliferative actions in fibroblast cells, J. Agric. Food Chem 44 (6) (1996) 1387–1394, https://doi.org/10.1021/jf950652k.

[51] C. Dipankar, S. Murugan, The green synthesis, characterization, and evaluation of the biological activities of silver nanoparticles synthesized from *Iresine herbstii* leaf aqueous extracts, Colloidssurf. b: Biointerfaces 98 (2012) 112–119, https://doi.org/10.1016/j.colsurfb.2012.04.006.

[52] F. Erci, R. Cakir-Koc, Rapid green synthesis of noncytotoxic iron oxide nanoparticles using aqueous leaf extract of *Thymbra spicata* and evaluation of their antibacterial, antibiofilm, and antioxidant activity, Inorg. Nano-Metal. Chem 51 (5) (2020) 683–692, https://doi.org/10.1080/24701556.2020.1802754.

[53] A. Ahmed, M.S. Javed, S. Khan, T.M. Almutairi, A.A.A. Mohammed, R. Luque, Green synthesized Ag decorated CeO_2 nanoparticles: Efficient photocatalysts and potential antibacterial agents, Chemosphere 310, 136841 https://doi.org/10.1016/j.chemosphere.2022.136841.

[54] V.V.T. Padil, M. Černík, Green synthesis of copper oxide nanoparticles using gum karaya as a biotemplate and their antibacterial application, Int. J. Nanomed. 8 (2013) 889–898, https://doi.org/10.2147/IJN.S40599.

[55] R.A. Ismail, G.M. Sulaiman, S.A. Abdulrahman, T.R. Marzoog, Antibacterial activity of magnetic iron oxide nanoparticles synthesized by laser ablation in liquid, Mater. Sci. Eng.: C 53 (2015) 286–297, https://doi.org/10.1016/j.msec.2015.04.047.

[56] T. Mosmann, Rapid colorimetric assay for cellular growth and survival: application to proliferation and cytotoxicity assays, J. Immunol. Methods 65 (1–2) (1983) 55–63, https://doi.org/10.1016/0022-1759(83)90303-4.

[57] R. Sever, J.S. Brugge, Signal transduction in cancer, Cold Spring Harb. Perspect. Med. 5 (4) (2015) a006098, 10.1101%2Fcshperspect.a006098.

[58] K.S. Khashan, G.M. Sulaiman, S.A. Hussain, T.R. Marzoog, M.S. Jabir, Synthesis, characterization, and evaluation of anti-bacterial, anti-parasitic and anti-cancer activities of aluminum-doped zinc oxide nanoparticles, J. Inorg Organomet. Polym. Mater. 30 (9) (2020) 3677–3693, https://doi.org/10.1007/s10904-020-01522-9.

[59] M.S. Kumar, N. Supraja, E. David, Photocatalytic degradation of methylene blue using silver nanoparticles synthesized from *Gymnema sylvestre* and antimicrobial assay, Novel. Res. Sci 2 (2) (2019) 1–7.

[60] U. Younas, A. Gulzar, F. Ali, M. Pervaiz, Z. Ali, S. Khan, Z. Saeed, M. Ahmed, A. A. Alothman, Antioxidant and oanic dye removal potential of Cu-Ni bimetallic nanoparticles synthesized using Gazania rigens extract, Water 13 (19) (2021), https://doi.org/10.3390/w13192653, 2653.